Hexagonal Petals-like Cobalt Oxide Nanowire Arrays Encapsulated by MOF-derived Co/N-codoped Carbon for Boosting Electrochemical Capacitor Behaviour

Xiao-Man Cao,[a,c] Zhi-Jia Sun*[a,c] and Zheng-Bo Han*[b]

[a] College of Chemistry and Materials Engineering, Bohai University, Jinzhou 121013, P.R. China. E-mail: sunzhijia@bhu.edu.cn.

[b] College of Chemistry, Liaoning University. Shenyang 110036, P.R. China. E-mail: ceshzb@lnu.edu.cn

[c] Liaoning Engineering Technology Research Center of Supercapacitor, Bohai University, Jinzhou 121013, P.R. China.

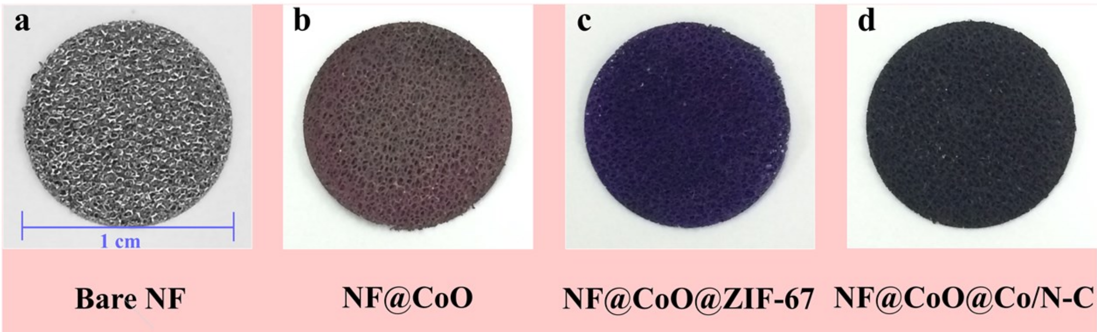

Figure S1. Photographs of the bare NF, NF@CoO, NF@CoO@ZIF-67 and NF@CoO@Co/N-C samples.

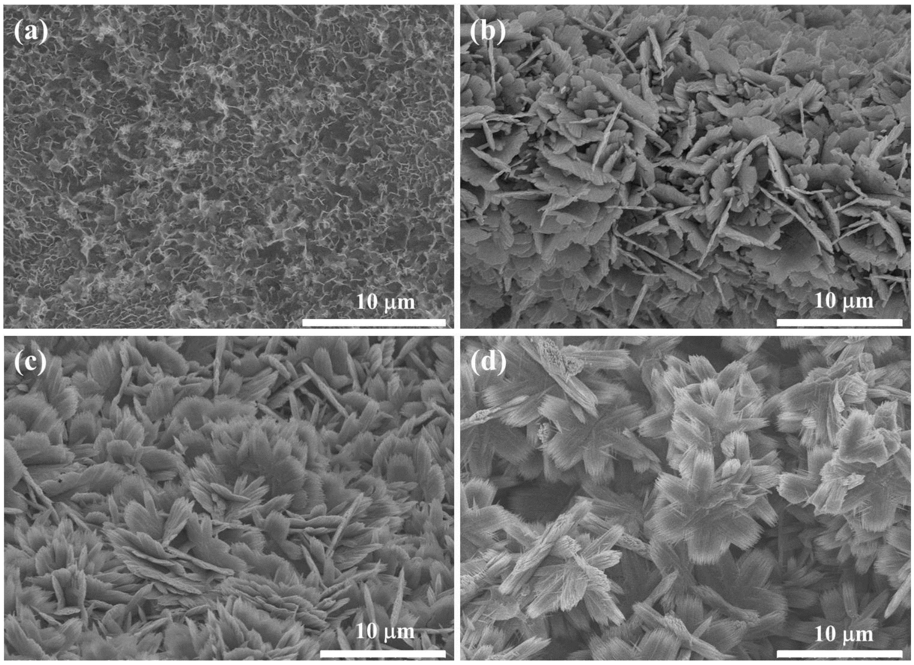

Figure S2. Formation process of nanowire-assembled hexagonal petals-like CoO. SEM images of CoO prepared at different reaction time length: (a) 10 min; (b) 1 h; (c) 5h; (d) 10 h.

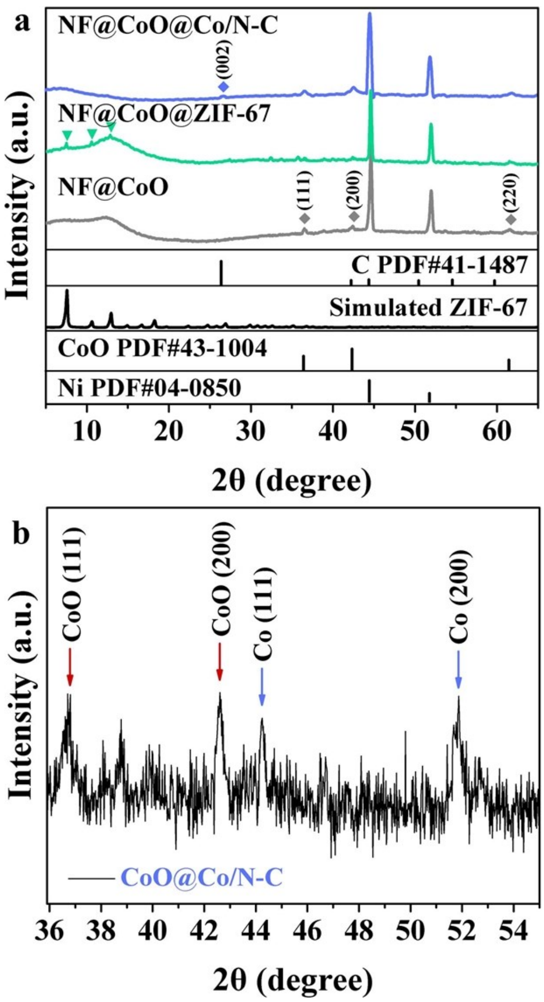

Figure S3. (a) PXRD patterns of NF@CoO, NF@CoO@ZIF-67 and NF@CoO@Co/N-C, (b) the enlarged PXRD pattern of CoO@Co/N-C powder sample without nickle foam.

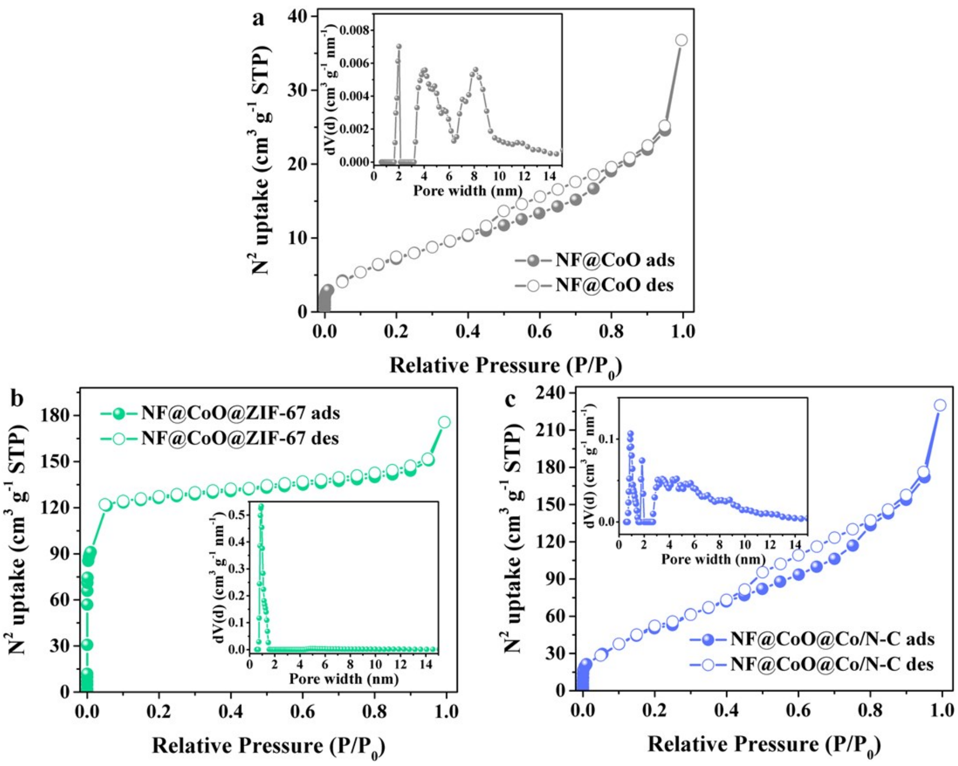

Figure S4. Nitrogen (77K) adsorption-desorption isotherms and pore size distribution for NF@CoO, NF@CoO@ZIF-67 and NF@CoO@Co/N-C.

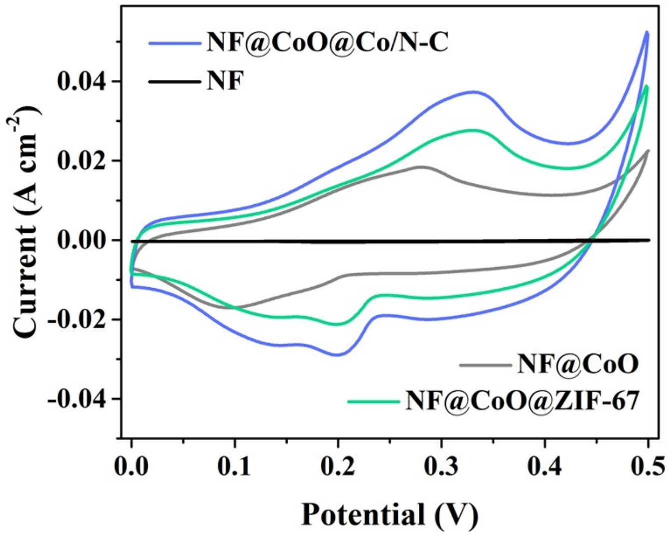

Figure S5. Cyclic voltammograms of bare NF, NF@CoO, NF@CoO@ZIF-67 and NF@CoO@Co/N-C at scan rate of 6 mV s^{-1}.

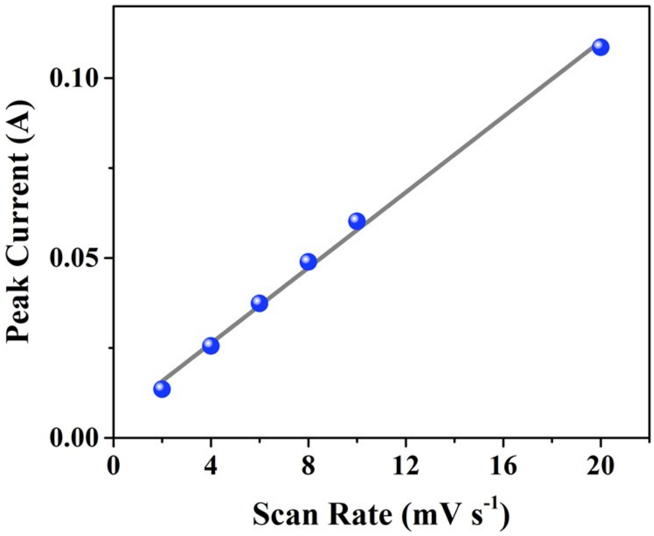

Figure S6. Relationship between anodic peak current and scan rate for NF@CoO@Co/N-C.

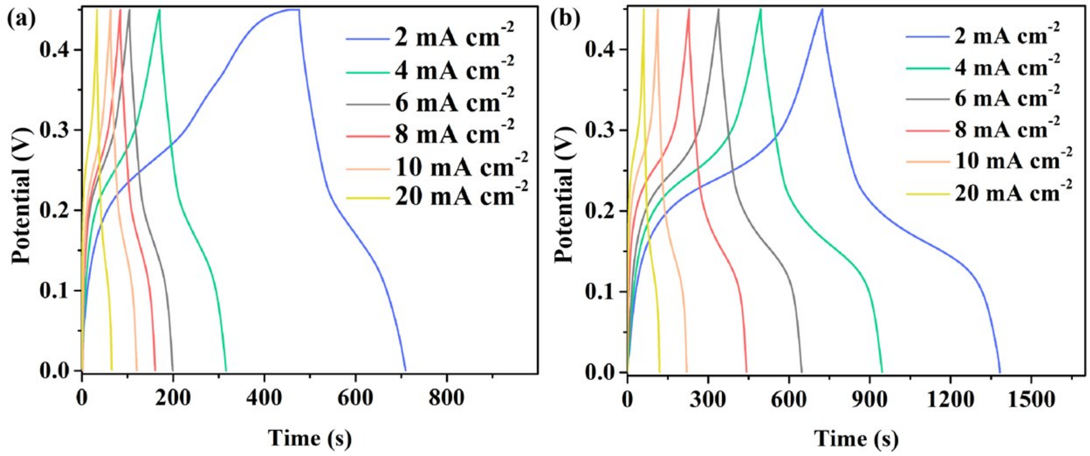

Figure S7. GCD curves recorded at different current densities from 2 to 20 mA cm^{-2} for (a) NF@CoO, (b) NF@CoO@ZIF-67.

Table S1. Comparison of capacitance and rate capability of NF@CoO@Co/N-C with recently reported cobaltous oxide-based electrodes.

Electrode	Current density/ Scan rate	Electrolyte	Capacitance	Rate capability
CoO[S1]	0.5 A g^{-1}	1 M KOH	600 F g^{-1}	0.5~16 A g^{-1} (32 times) 69.3%
Co_3O_4@CoO@carbon[S2]	1 A g^{-1}	1 M KOH	324 F g^{-1}	1~10 A g^{-1} (10 times) 63. 9%
Co_3O_4@CoO[S3]	0.2 A g^{-1}	6 M KOH	362.8 F g^{-1}	0.2~4 A g^{-1} (20 times) 78.7%
Co_3O_4@CoO@Co@C[S4]	2 A g^{-1}	1 M KOH	370 F g^{-1}	1~40 mV s^{-1} (40 times) 64%
CoO/Co_9S_8@CN[S5]	0.5 A g^{-1}	6 M KOH	303.3 F g^{-1}	0.5~5 A g^{-1} (10 times) 70.0%
$CoCO_3$@CoO[S6]	1 A g^{-1}	1 M KOH	0.77 F cm^{-2} 510 F g^{-1}	0.2~10 A g^{-1} (50 times) 82.0%
CoO nanowall[S7]	1 A g^{-1}	6 M KOH	352 F g^{-1}	1~20 A g^{-1} (20 times) 72.7%
CoO@MnO_2[S8]	2 mA cm^{-2}	6 M KOH	2.40 F cm^{-2}	2~20 mA cm^{-2} (10 times) 57.5%
C/CoO-200[S9]	0.5 A g^{-1}	2 M KOH	207 F g^{-1}	0.5~10 A g^{-1} (20 times) 79.6%
CoO@MnO_2 NNAs[S10]	2 mA cm^{-2}	6 M KOH	3.03 F cm^{-2}	2~20 mA cm-2 (20 times) 46.9%
NF@CoO*	**2 mA cm^{-2}**	**6 M KOH**	**2.32 F cm^{-2}**	**2~20 mA cm^{-2} (10 times) 52.2%**
NF@CoO@ZIF-67*	**2 mA cm^{-2}**	**6 M KOH**	**3.13 F cm^{-2}**	**2~20 mA cm^{-2} (10 times) 71.2%**
NF@CoO@Co/N-C*	**2 mA cm^{-2}**	**6 M KOH**	**5.61 F cm^{-2}** **1693.4 F g^{-1}**	**2~20 mA cm^{-2} (10 times) 91.3%**

***This work**

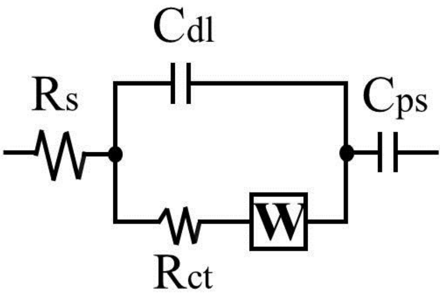

Figure S8. The equivalent circuit mode for the Nyquist plots of NF@CoO, NF@CoO@ZIF-67 and NF@CoO@Co/N-C.

The equivalent circuit for the Nyquist plots of the samples is shown in Figure S8. The semicircle and linear region indicate the charge-transfer resistance (R_{ct}) and Warburg impedance (W), which indicates ion diffusion/transport from the electrolyte to the electrode surface. The intercept with the real axis (Z_{Re}) at high frequency indicates electrolyte resistance (R_s). C_{dl} is the double layer capacitance and C_{ps} is the pseudocapacitance.

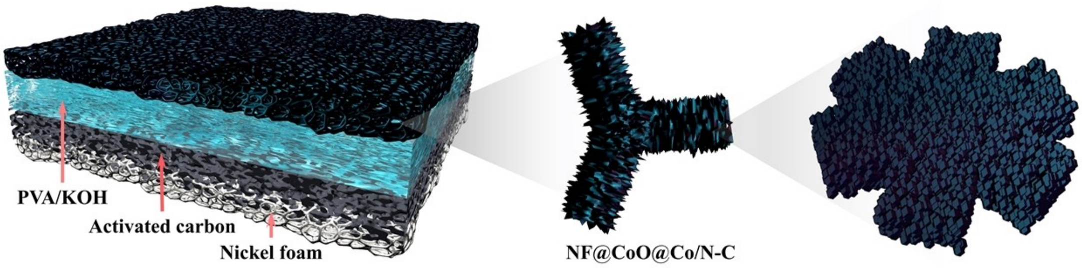

Figure S9. Schematic representation of the ASC device by using NF@CoO@Co/N-C cathode, actived carbon (AC) anode, and PVA/KOH gel as electrolyte.

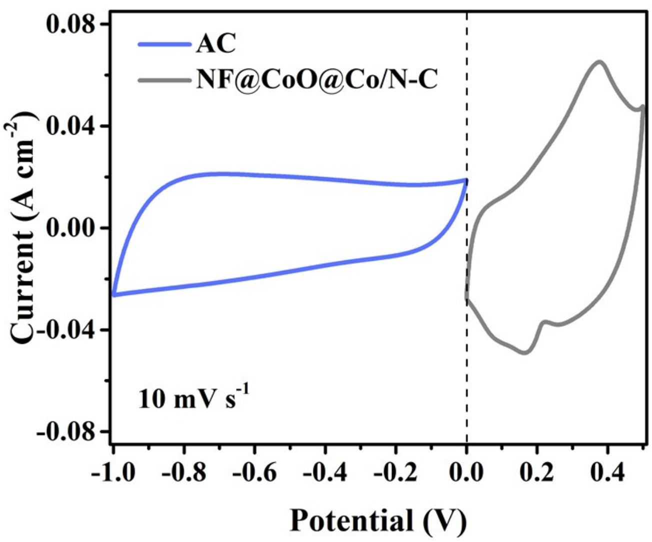

Figure S10. CV curves collected for NF@CoO@Co/N-C and AC electrodes at a scan rate of 10 mV s^{-1}.

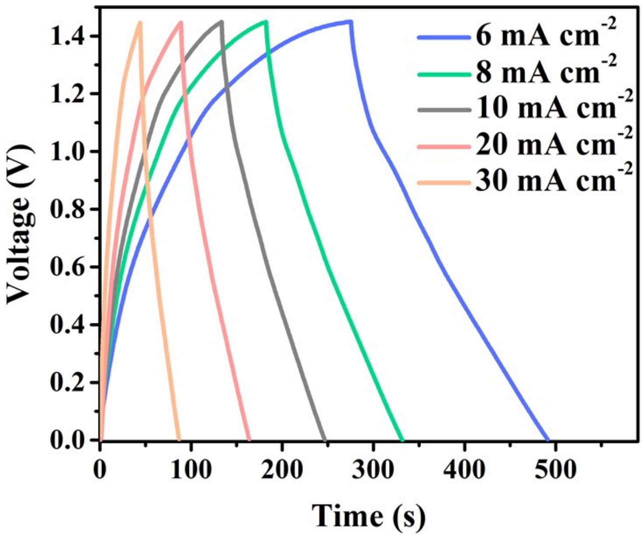

Figure S11. GCD curves of the ASC device at different current densities.

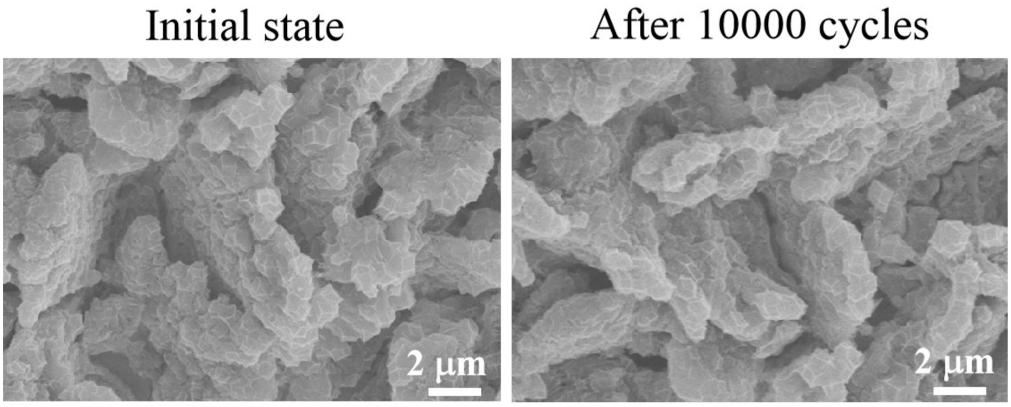

Figure S12. SEM images of NF@CoO@Co/N-C before and after 10000 cycles.

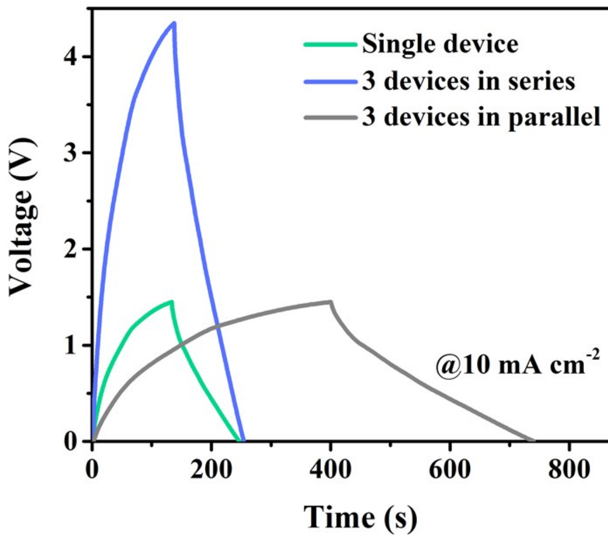

Figure S13. GCD curves of the ASC devices connected in series and in parallel.

Supporting references

(1) C. Zheng, C. B. Cao, Z. Ali, J. H. Hou, *J. Mater. Chem. A*, 2014, **2**, 16467-16473.

(2) E. Duraisamy, H. T. Das, A. S. Sharma, P. Elumalai, *New J. Chem.*, 2018, **42**, 6114-6124.

(3) J. C. Deng, L. T. Kang, G. L. Bai, Y. Li, P. Y. Li, X. G. Liu, Y. Z. Yang, F. Gao, W. Liang, *Electrochimica Acta*, 2017, **132**, 127-135.

(4) D. Y. Xu, C. P. Mu, J. Y. Xiang, F. S. Wen, C. Su, C. X. Hao, W. T. Hu, Y. F. Tang, Z. Y. Liu, *Electrochimica Acta*, 2016, **220**, 322-330.

(5) C. Shi, M. W. Chen, X. Han, Y. F. Bi, L. L. Huang, K. Zhou, Z. P. Zheng, *Inorg. Cherm. Front.*, 2018, **5**, 1329-1335.

(6) X. Ji, S. Cheng, L. F. Yang, Y. Jiang, Z. J. Jiang, C. H. Yang, H. Zhang, M. L. Liu, *Nano Energy*, 2015, **11**, 736-745.

(7) N. Tang, W. Wang, H. H. You, Z. J. Zhai, J. Hilario, L. Zeng, L. Zhang, Catal. Today. https://doi.org/10.1016/j.cattod.2018.03.024

(8) X. Z. Wang, Y. H. Xiao, D. C. Su, S. G. Xu, L. M. Zhou, S. D. Wu, L. F. Han, S. M. Fang, S. K. Cao, 2016, *Int. J. Hydrogen Energy*, 2016, **41**, 13540-13548.

(9) J. Y. Long, Z. S. Yan, Y. Gong, J. H. Lin, *Appl. Surf. Sci.*, 2018, **448**, 50-63.

(10) X. Z. Wang, Y. H. Xiao, D. C. Su, L. M. Zhou, S. D. Wu, L. F. Han, S. M. Fang, S. K. Cao, *Electrochimica Acta*, 2016, **194**, 377-384.